Resonance properties of metallic ring systems

We review our recent efforts in understanding the resonance properties of metallic ring systems using a rigorous mode-expansion theory. In the quasi-static limit, we established a matrix-form circuit equation to calculate the frequencies and current distributions for all resonance modes in a ring system. We then applied the theory to study different split ring resonators (SRR). We show that the circuit equations can be analytically solved in the thin-wire limit. Our theoretical results were all successfully verified by finite-different-time-domain simulations on realistic systems and available experiments.

Lei Zhou[1]*, Xueqin Huang[1], Yi Zhang[1], Siu-Tat Chui[2]

[1]Surface Physics Laboratory (State Key Laboratory) and Physics Department, Fudan University, Shanghai 200433, P. R. China

[2]Bartol Research Institute, University of Delaware, Newark, Delaware 19716, USA

** Email: phzhou@fudan.edu.cn*

Introduction

In 1968, Veselago[1] proposed that a medium with simultaneously negative permittivity and permeability possesses a negative refractive index, and exhibits many unusual electromagnetic (EM) properties. This proposal did not attract immediate attention since it is well accepted that a natural material shows no magnetism at high frequencies[2]. A breakthrough appeared in 1999 when Pendry[3] showed that a split ring resonator (SRR) could provide magnetic responses at any desired frequency. People then successfully fabricated metamaterials by combining magnetic resonators and electric wires, and demonstrated many unusual EM phenomena based on metamaterials, such as the negative refraction[4-10], the super focusing[11-14] and the subwavelength cavity[15-17]. Scientists continued to explore other extraordinary EM phenomena related to metamaterials, including the unusual photonic bandgap effects[18-20], the invisibility cloaking[21-23], the unusual nonlinear effects[24-29], etc. When the concept of metamaterial was pushed to optical frequencies, other magnetic resonant structures were proposed, such as the rod-pair structure[30, 31], the fishnet structures[9, 32, 33], and a circular array of nano-spheres[33-35].

As the first realization of artificial magnetism, the SRR structures naturally attracted the most extensive attention. People have studied the circular SRRs[3, 4, 6, 36-53], the rectangular SRRs[5, 54-68], SRRs with different cross-sections, metal line widths, metal thicknesses, and substrates[6, 36, 55, 60, 61], SRRs with different numbers of splits[36, 37, 56], and different numbers of rings[48, 64], and so on. Some applications were also proposed for the SRR. For instance, researchers proposed to use SRRs as antennas[69] and as couplers for channel dropping[70], inserted SRRs into a cut-off waveguide to enhance transmissions[71, 72],

ISSN:1369 7021 © Elsevier Ltd 2009

and used SRRs as lenses for imaging[73, 74]. Some groups attempted to scale down the size of SRR to realize artificial magnetism at higher frequencies[4-6, 57, 58, 63, 75]. However, the scaling does not always work, and the increase of resonance frequency will saturate under certain conditions[56, 60]. Some other groups tried to tune the resonance frequency of a SRR, by inserting additional capacitance in the ring gaps[36, 39], using photocapacitance of the semi-insulating GaAs in the gap[38], and combining the SRRs with nematic liquid crystals[62]. Recently, the designs and fabrications of isotropic metamaterials based on SRRs began to draw intensive attentions[76-82].

Many theoretical efforts were devoted to understanding the exotic EM wave properties of the SRR structures. In a pioneering paper, Pendry ***et al.***[3] analyzed the resonance properties of a SRR by assuming a metallic ring as a single lumped element with empirical circuit characteristics. Later, Shamonin ***et al.***[42] considered more inductive/capacitive effects by assuming the SRR to consist of an infinite number of lumped circuit elements. Many other analytical methods were developed to study the properties of the SRRs[41, 43-46, 48, 49, 64, 65] from various aspects. However, in all these approaches, the inductive/capacitive effects in the rings were not completely considered. In addition, all these approaches need a set of empirical circuit parameters that cannot be calculated rigorously. Those empirical parameters were usually determined under some approximations[3, 42]. The SRR systems were also studied by numerical calculations[54, 55, 61, 62, 66-68]. Although such full-wave studies contain all relevant field information, it is sometimes difficult to extract useful properties of a SRR, such as the bi-anisotropy polarizabilities, from the obtained information.

In reviewing these efforts, we find that an analytical approach on more rigorous ground is highly desirable to study the metallic ring systems. In this paper, we review our recent efforts to establish such a theory, with inductive/capacitive effects fully included and all circuit parameters calculated rigorously, to study the EM properties of various metallic ring systems[50-53]. We first briefly review the theoretical developments in next section, and then present the applications of our theory to several typical SRR systems. We finally summarize our results in the last section.

Theoretical developments of the mode-expansion theory

Basic theory for a single-ring

We consider a single ring of radius R in the xy-plane, as shown in Fig. 1a[50]. In what follows, a common time-varying factor $\exp(i\omega\tau)$ is omitted for every quantity. In the quasi-static limit, the inductive field $\vec{E}_L(\vec{r})$ and the capacitive field $\vec{E}_C(\vec{r})$ can be expressed as

$$\vec{E}_L(\vec{r}) = -i\omega\mu_0 \int \vec{j}(r')d\vec{r}'/(4\pi\,|\vec{r}-\vec{r}'|),$$

$$\vec{E}_C(\vec{r}) = \frac{1}{i\omega}\frac{1}{4\pi\varepsilon_0}\nabla\int\left[\nabla'\cdot\vec{j}(\vec{r}')\right]d\vec{r}'/|\vec{r}-\vec{r}'|$$

where $\vec{j}(\vec{r}')$ describes the current flowing in the wire. Suppose that the wire has a circular cross-section with a radius a and $a << R$, the current distribution can be written as $\vec{j}(\vec{r}') = \vec{e}_\phi I(\phi)\sin\theta\delta(\cos\theta)\delta(r'-R)/R$ with $\vec{e}_\phi = -\sin\phi\vec{e}_x + \cos\phi\vec{e}_y$. We expand every physical quantity as a Fourier series,

$$I(\phi) = \sum^{+\infty} I_m e^{im\phi}\ ,\ \vec{E}_{L,C}(\phi)\cdot\vec{e}_\phi = \sum^{+\infty} E^m_{L,C} e^{im\phi}\ . \tag{1}$$

Then we carry out the integrations in $\vec{E}_L(\vec{r}), \vec{E}_C(\vec{r})$ to obtain

$$E^m_L = -i\omega L_m I_m\,,\ E^m_C = -I_m/(i\omega C_m) \tag{2}$$

where the circuit parameters are defined by

$$L_m = \mu_0(A_{m-1} + A_{m+1})/4\,,\quad C_m^{-1} = m^2 A_m/\left(2\varepsilon_0 R(R-a)\right) \tag{3}$$

Here the key function is

$$A_m = \sum_{l=|m|}^{\infty}\frac{(l-m)!}{(l+m)!}\alpha^l\left[P_l^m(0)\right]^2 \tag{4}$$

in which P_l^m is the associated Legendre function and $\alpha = (R-a)/R<1$. In the thin-wire limit (a << R), we found an asymptotic form. This logarithmic $A_m \approx D_m - \ln(2a/R)/(\alpha^m\pi)$ divergence is a typical

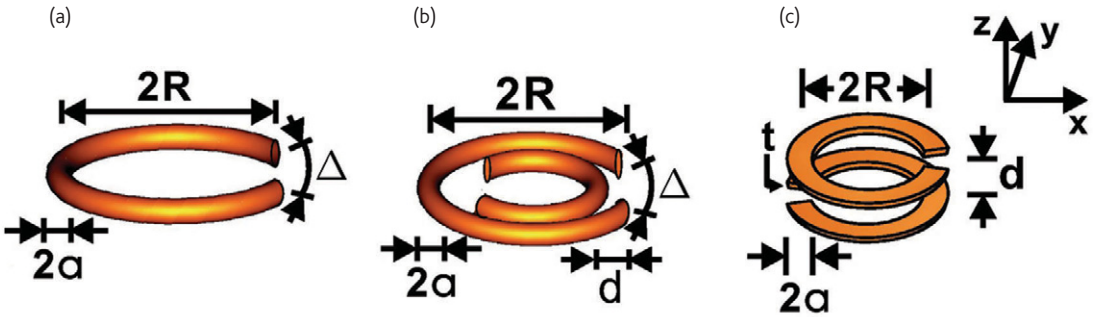

Fig. 1 Geometries of (a) single SRR, (b) co-planar SRR, and (c) BC-SRR.

characteristic of a thin-wire system[83]. Ohm's law tells us that $\vec{j}(\vec{r}) = \rho(\vec{r})\left[\vec{E}_L(\vec{r}) + \vec{E}_C(\vec{r}) + \vec{E}_{ext}(\vec{r})\right]$ where $\vec{E}_{ext}(\vec{r})$ is the external field and $\rho(\vec{r})$ is the resistivity function of the ring. In terms of the Fourier components, we get the following matrix equation,

$$\sum_{m'} H_{mm'} I_{m'} = E^m_{ext}, \tag{5}$$

where $H_{mm'} = \tilde{\rho}(m-m') + i\omega L_m\left(1-\Omega_m^2/\omega^2\right)\delta_{mm'}$; $\tilde{\rho}(m-m')$ is the Fourier component of $\tilde{\rho}(\phi) = \rho(\phi)/S$ (S is the wire cross-section area) and $\Omega_m = 1/\sqrt{L_m C_m}$. Diagonalizing the **H** matrix, we obtain the eigenvalues $\{\lambda_j\}$ and eigenvectors of all EM modes, from which we can calculate the resonance frequencies, induced EM dipole moments, and the polarizabilities and the bi-anisotropic polarizabilities. For example, all resonance frequencies ω_j of the SRR are obtained through solving the equation

$$\det[H_{mm'}(\omega)] = \Pi_m \lambda_m(\omega) = 0 \tag{6}$$

Extensions to other situations

The above mode-expansion theory can be easily extended to more complex situations. For the two ring systems, we find that the matrix-circuit equation could be written as

$$\sum_{m'j'} H_{\{mj\},\{m'j'\}} I_{m'j'} = E^{ext}_{mj} \tag{7}$$

where the matrix elements are

$$H_{\{mj\},\{m'j'\}} = \rho_j(m-m')\delta_{jj'} + i\left(\omega L_m^{jj'} - \frac{1}{\omega C_m^{jj'}}\right)\delta_{mm'}. \tag{8}$$

Here j, j' = 1, 2 label the two rings, L_m^{jj} and C_m^{jj} are the self inductive/capacitive parameters and $L_m^{jj'}$ and $C_m^{jj'}$ are the mutual inductance/capacitance parameters. The above theory can be applied to study the coplanar double-ring SRR in which two rings are placed on the same plane but with different radii (Fig. 1b), and the broadside coupled SRR (BC-SRR) with two identical rings placed on different planes (Fig. 1c). In addition, the gap position of each ring can be arbitrary in our system, which is simply described by the resistivity function $\rho(\phi)$. It is straightforward to extend our theory to study multi-ring systems. For the detailed forms of those circuit parameters, please refer to the original publications[51, 52].

Strictly speaking, the theory presented so far is only applicable to rings formed by thin wires with circular cross-sections. In practical situations, the metallic rings often have rectangular cross-sections[3-6, 36-49, 54-68], where the delta-like current distribution is no longer reasonable. Suppose the wire's cross-section is defined as *tx2a*, where *2a* and *t* are the width and thickness of the wire, we focus on the flat-wire case satisfying $R >> 2a >> t$. For a good metal, the skin effect dictates that the current should mainly distribute on the metal surface. Noting that $a << \lambda$ with λ being the wavelength of the probing EM wave of interest, we further assume that the current distributes uniformly along the wire width. Therefore, the current distribution in the flat wire can be written as,

$$\vec{j}(\vec{r}) = \begin{cases} j(\phi)\cdot t_\delta\left[\delta(z+t/2)+\delta(z-t/2)\right]\vec{e}_\phi, & \rho \in [R-a, R+a] \\ 0, & \text{otherwise} \end{cases} \tag{9}$$

where $t_\delta << t$ is the skin depth of the metal. We average both $\vec{E}_{L,C}(\vec{r})$ and $\vec{j}(\vec{r}')$ over the cross-section area of the wire, and then set up the relationship between the two averaged quantities. For example, the averaged inductive field is

$$\bar{\vec{E}}_L(\phi) = \frac{\int \vec{E}_L(\rho, z, \phi)\cdot\vec{e}_\phi t_\delta\left[\delta(z+t/2)+\delta(z-t/2)\right]dzd\rho}{\int t_\delta\left[\delta(z+t/2)+\delta(z-t/2)\right]dzd\rho}. \tag{10}$$

and the total current is given by $I(\phi) = j(\phi).4at_\delta$. By linking these two averaged quantities, we can calculate the relevant circuit parameters[52]. Therefore, the circuit equations (5), (7) are still correct for flat-wire SRR cases, but with a set of modified circuit parameters[52].

Applications and discussions

Our theory can be applied to study the resonance properties of various metallic ring systems. In the following three subsections, we summarize our results on a single-ring SRR, a coplanar double-ring SRR, and a BC-SRR, correspondingly.

Single-ring SRR

Consider a single-ring SRR illustrated in Fig. 1a. In the microwave frequency regime, we can safely set the resistivity of the metal as 0, and that of the air-gap as *r*. We will let $r\to\infty$ in the end. The magnitude of the lowest eigenvalue of matrix **H** is shown as a function of frequency in Fig. 2 for a typical SRR. The series of resonances in Fig. 2 can be categorized into two classes. The even-numbered resonances ω_{2m} coincide well with the intrinsic resonances Ω_m, which in the thin-wire limit ($a/R\to 0$) becomes $\Omega_m \to m\omega_u$ where $\omega_u = c/R$ is the frequency unit of the present problem. Noting that $\lambda_{2m} = 2\pi c/\omega_{2m} = m.2\pi R$, we find that these resonances are solely determined by the ring geometry, with currents forming standard standing waves in the ring. The odd-numbered ones, however, must be introduced by the air gap Δ.

In fact, these resonance frequencies can be calculated analytically in the following limits: (1) $\Delta\to 0$; (2) $a/R\to 0$; (3) metal is perfect and the gap is ideal insulator ($r\to\infty$). Under these conditions, we have *rigorously* solved the matrix problem (6) and found two sets of solutions[53]. One set of resonance frequencies is

$$\omega_{2m} = m\omega_u, \qquad m = 1, 2, \ldots \tag{11}$$

with eigenvectors exhibiting odd-symmetries (i.e., $I_{-m} = -I_m$). These modes correspond to the even-numbered resonance modes as shown in Fig. 2. Another set of resonance modes are determined by the following polynomial equation,

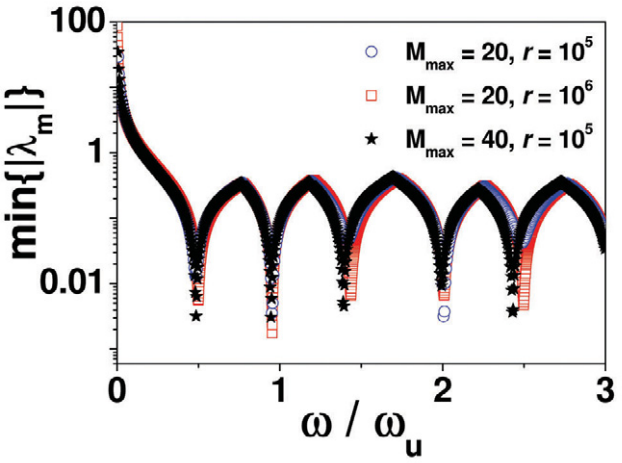

Fig. 2 min[$|\lambda_m|$] as functions of ω/ω_u for a single-ring SRR with $\Delta = \pi/40$ and $\alpha = 0.99$, calculated with different values of M_{max} (the cutoff value of m) and r (in units of $\mu_0\omega_u$). Reproduced from[50] with permission from the American Physical Society.

$$1+\sum_{m=1}^{\infty}\frac{2L_0\omega^2}{L_m\omega^2-1/C_m}=0 \qquad (12)$$

and their eigenvectors exhibit even symmetry (i.e., $I_{-m} = -I_m$). Since as $a/R\to 0$, we have $L_m\to\ln(R/a)$ and $1/C_m\to m^2\ln(R/a)$, using the identity

$$k\pi\cot(k\pi)=1+\sum_{m=1}^{\infty}2k^2/(k^2-m^2),$$

we found that Eq. (12) can be written as $(\omega/\omega_u)\cot(\omega\pi/\omega_u) = 0$, leading to the following solutions

$$\omega_{2m+1} = (m + 1/2)\omega_u, \qquad m = 0, 1, 2,... \qquad (13)$$

These solutions are just the odd-numbered resonance modes depicted in Fig. 2.

The information of the eigenvectors enables us to evaluate the EM responses of the system. Consider different probing plane waves with (a) $\vec{E}\parallel\hat{y},\vec{k}\parallel\hat{z}$, (b) $\vec{E}\parallel\hat{y},\vec{k}\parallel x$, (c) $\vec{E}\parallel\hat{x},\vec{k}\parallel\hat{z}$, (d) $\vec{E}\parallel\hat{x},\vec{k}\parallel y$, we show in Fig. 3 the induced dipole moments as functions of frequency. The odd-numbered resonance modes possess both magnetic (m_z) and electric (p_y) responses, while the even-numbered ones only electric (p_x) responses. The appearance of p_y is always accompanied by the appearance of m_z, manifesting the bi-anisotropy property of the SRR[43, 47, 49]. Symmetry restricts a probing field to excite only a particular set of resonance modes of the SRR, and therefore, not all the resonance peaks appear simultaneously in each spectrum. We have performed finite-difference time-domain (FDTD) simulations[84] to verify these theoretical results. We first calculated the transmission spectra through arrays of such realistic SRR's, and then identify all resonance modes from the dips in the spectra. The transmission spectra under the four plane wave inputs are shown respectively in Fig. 4a-d. When we compare Fig. 4 with Fig. 3, we find that they agree with each other

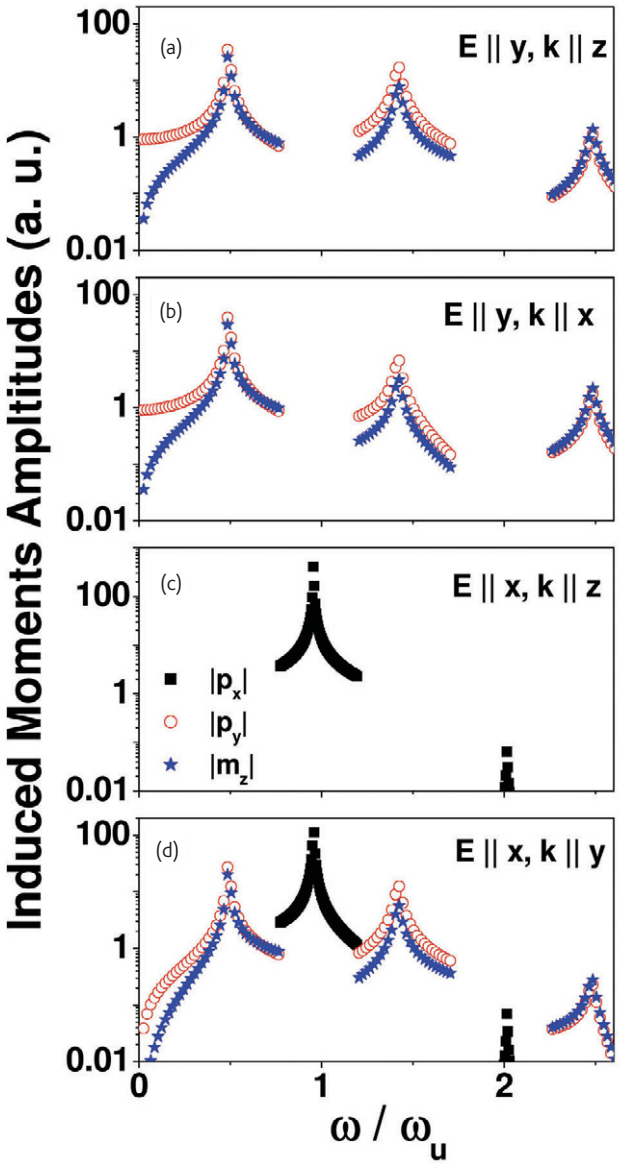

Fig. 3 Amplitudes of the induced moments, $|p_x|$, $|p_y|$, $|m_z|$, of the SRR as functions of ω/ω_u for different probing fields as shown in the figure. Reproduced from[50] with permission from the American Physical Society.

quite well. We clearly identify the dips at $\omega \approx 0.42\omega_u$ shown in Fig. 4a, b, d as the lowest eigen resonance mode (ω_1), the dips at $\omega \approx 1.19\omega_u$ shown in Fig. 4c, d as the second resonance mode (ω_2), and the dips at $\omega \approx 1.46\omega_u$ as the third one (ω_3). The quantitative differences between analytical and FDTD results must be caused by the couplings between different SRRs, since we have to adopt periodic arrays of SRRs to study the transmission spectra in the FDTD simulations.

Coplanar double-ring SRR

Now consider the coplanar double-ring SRR as shown in Fig. 1b. Suppose the two rings have radius $R_1 = R$, $R_2 = R - d$, and each wire has

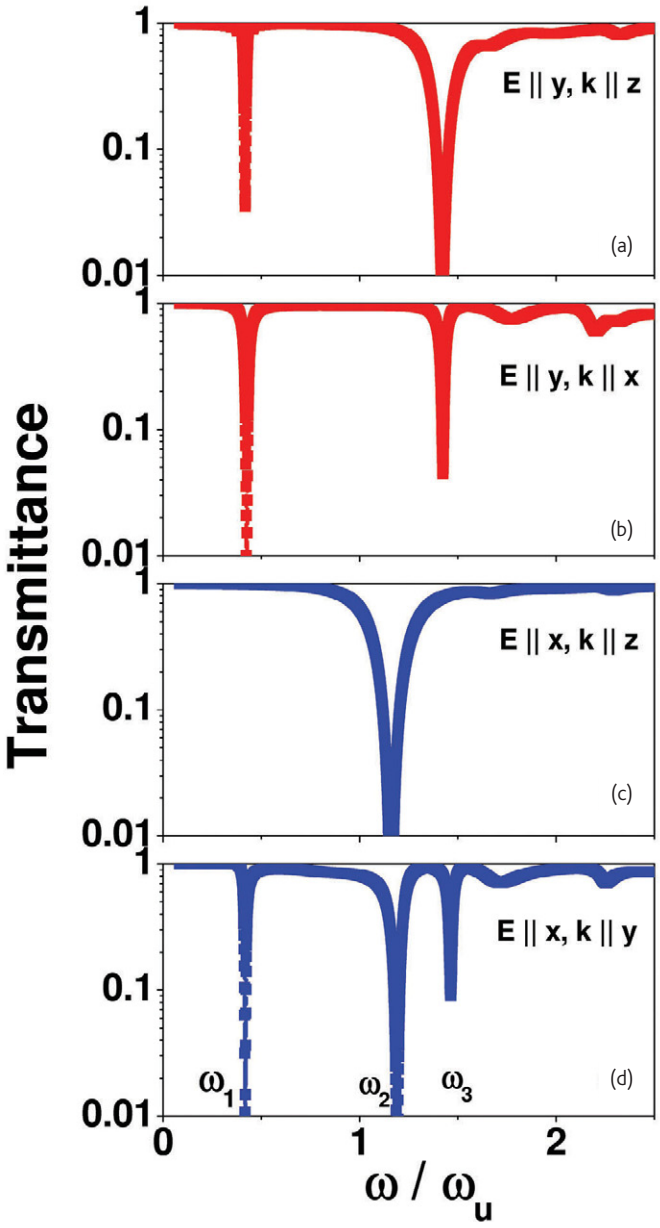

Fig. 4 FDTD calculated transmission spectra of the SRR arrays as functions of ω/ω_u for plane wave inputs specified in the figure. Here the SRR has R = 4 mm, a = 0.1 mm, and $\Delta = \pi/40$. Reproduced from[50] with permission from the American Physical Society.

a radius $a_1 = a_2 = a << R$. For an example with structural details shown in the caption of Fig. 5, we solved the matrix equation (7) and showed in Fig. 5 the calculated $\min[|\lambda_l|]$ as a function of ω/ω_u. Compared with the spectra of a single-ring SRR shown in the same figure, we find that each single-ring mode has split into a pair of modes in the double-ring case through mutual inductance/capacitance effects. Such inter-ring interactions may combine components of different rings with a certain relative phase to form a double-ring eigenmode[51]. Therefore, the magnetic (electric) polarizations are highly diminished in the ω_1^H (ω_1^L)

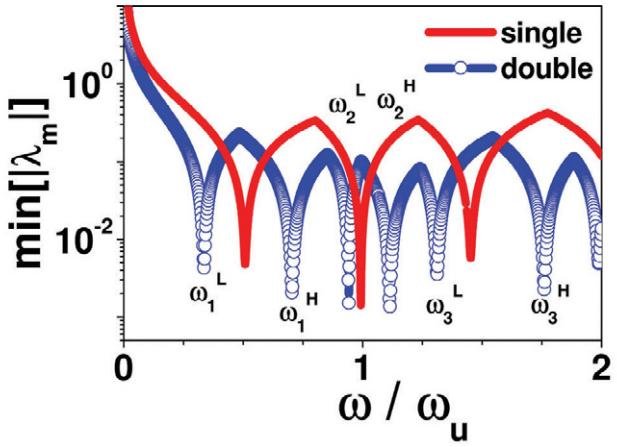

Fig. 5 $\min[|\lambda_l|]$ (in arbitrary units) as the functions of ω/ω_u calculated for a double-ring SRR (symbols) with R = 4 mm, d = 0.4 mm, $a = 0.1\sqrt{\pi}$ mm, $\Delta = \pi/90$, and a single-ring SRR (lines) with R = 3.8 mm, $a = 0.1\sqrt{\pi}$ mm, $\Delta = \pi/90$. Reproduced from[51] with permission from the American Institute of Physics.

mode, and as the results, the bi-anisotropy is also highly suppressed as two rings approach.

Fig. 6 shows the dipole moments of the structure induced by different external plane waves. Similar to the single-ring case (Fig. 3), we find that the odd-numbered modes (ω_1^L, ω_1^H, ω_3^L, ω_3^H,...) carry both electric (P_y) and magnetic (M_z) polarizations, while the even-numbered ones (ω_2^L, ω_2^H, ω_4^L, ω_4^H,...) carry only electric (P_x) polarizations. In particular, one may easily find that m_z is much stronger than p_y for the mode ω_1^L, but things become reversed for the mode ω_1^H. These are precisely the evidence of the polarization decreasing effects discussed above. We performed FDTD simulations[84] to calculate the transmission spectra through arrays of realistic SRR structures, and again the transmission dips in the spectra show excellently one-by-one correspondence to the moment peaks in Fig. 6[51].

The present theory allows us to *quantitatively* examine the bi-anisotropy of the SRR. We derived all elements of the electric/magnetic polarizabilities of the structure[51], following the definitions in[43, 47, 49]. We showed in Fig. 7a-b the calculated values of electric polarizability (α_{yy}^{ee}) and bi-anisotropic polarizability (α_{yz}^{em})[43, 47, 49], respectively, for double-ring SRR's with different values of *d*. Clearly, both α_{yy}^{ee} and α_{yz}^{em} are significantly suppressed as *d* decreases. As a result, such a mode becomes *purely magnetic* in the limit of $d \to 0$.

The magnetic resonance frequency ω_1^L is drastically lowered compared to the single-ring mode (denoted by ω_1). Under the condition $d >> a$, we applied a perturbation theory with a 3-mode approximation to derive the following analytical formula to quantitatively account for such a frequency shift[51],

$$\omega_1^L \approx \omega_1[1\text{-}2\ln(2d/R) / (3\ln(2a/R))]. \quad (14)$$

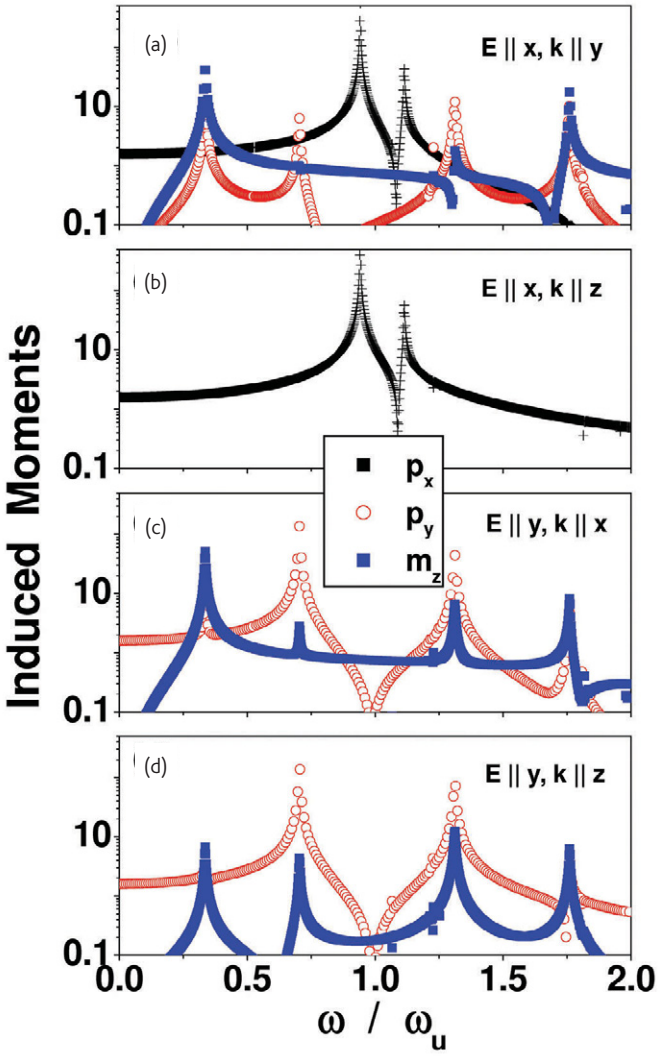

Fig. 6 Dipole moments (in arbitrary units) of the double-ring SRR (same as Fig. 5) induced by external plane waves with $\vec{E}$ and $\vec{k}$ directions specified in the legends. Reproduced from[51] with permission from the American Institute of Physics.

The physics behind (14) is that $\delta\omega/\omega_1$ is dictated by a competition between the mutual interaction ($\propto\ln(2d/R)$) and the self interaction ($\propto\ln(2a/R)$). FDTD simulations[51] on realistic SRR structures excellently verified the analytical formula (14).

This formula can also account for experiments very well. For the series of SRR's studied experimentally[36], adopting their definitions (i.e., set $R = r\text{-}w/2$, $a = w/2$, $d = t+w$ where w is the metal line width and t is the gap distance between two rings[36]) and taking the experimental data $\omega_1 = 2\pi$x4.58GHz[36], we get an expression,

$$f = 4.58[1\text{-}2\ln(2(t+w)/(r\text{-}w/2))/[3\ln(w/(r\text{-}w/2))]] \qquad (15)$$

to estimate the resonance frequencies of SRR's measured[36]. Fig. 8 shows that the experimental data[36] are reasonably described by (15).

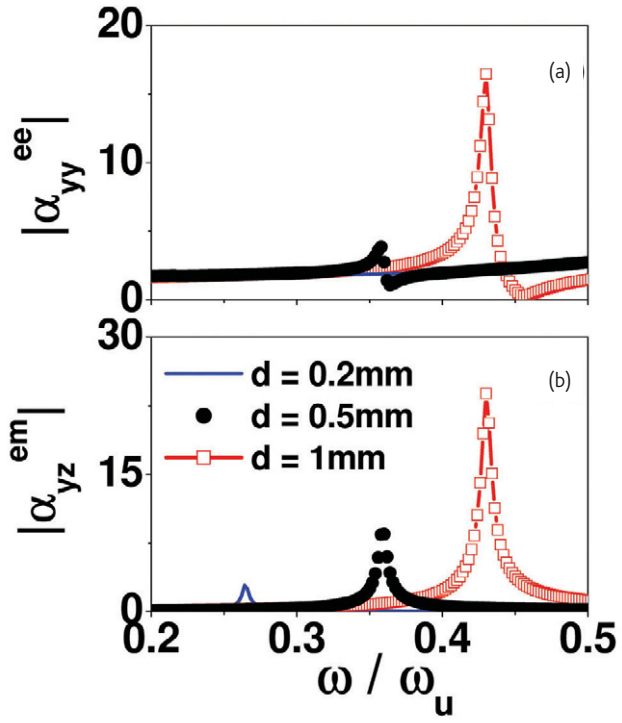

Fig. 7 Amplitudes of (a) electric polarizability $|\alpha^{ee}_{yy}|$ and (b) bi-anisotropic polarizability $|\alpha^{em}_{yz}|$ as the functions of ω/ω_u, for double-ring SRR's with $R = 4$ mm, $a = 0.1\sqrt{\pi}$ mm, and different values of d specified in the legend. Reproduced from[51] with permission from the American Institute of Physics.

BC - SRR

We now consider the BC-SRR as shown in Fig. 1c. The spectrum of resonance frequency in the BC-SRR case is quite similar to that of a coplanar SRR (see Fig. 5), and each single-ring mode has again split into a pair of modes with different symmetries[52]. However, we found that the dipole moments exhibited by the resonance modes in a BC-SRR[52] are quite different from those in the coplanar SRR[51]. In particular, in addition to the perpendicular magnetic polarization m_z, two more in-plane polarizations m_x, m_y can also be induced for the BC-SRR under specific conditions. We summarized the characteristics of the EM polarizations for the lowest four modes in Table 1. Two important conclusions can be drawn. First, all the resonance modes in a BC-SRR are *completely free of bi-anisotropy* (i.e., either *purely* magnetic or *purely* electric). This important character has also been noted previously[43, 47, 49]. Second, some resonance modes (say, ω_1^L) could possess two magnetic moments simultaneously.

The second property of the BC-SRR enables us to design a *super* resonance unit for metamaterials. Metamaterials that possess magnetic responses along all three dimensions drew much attention recently[76-82]. As many resonant structures are inherently anisotropic, a standard method to design 3D magnetic materials is to rotate the unite cell element and combine it with the original one to form an isotropic unit cell[76-82]. Recently, several non-SRR-based schemes were also

Table 1 Characteristics of electric/magnetic polarizations of low-lying modes for a BC-SRR and a single-ring SRR. Reproduced from[52] by permission of the American Physical Society.

System	Mode	p_x	p_y	m_z	m_x	m_z
Single	ω_1	No	Yes	Yes	No	No
Double	ω_1^L	No	Disappear	Enhanced	***New***	No
	ω_1^H	No	***Enhanced***	Disappear	No	No
Single	ω_2	Yes	***No***	No	No	No
Double	ω_2^L	Enhanced	***No***	No	No	No
	ω_2^H	Disappear	***No***	No	No	***New***

proposed to fabricate 3D isotropic metamaterials[85-88]. Here, we provide an alternative approach. We demonstrate that a layered structure, composed by planar arrays of BC-SRR's, can exhibit magnetic responses along all three dimensions at the same frequency. Since the structure is basically a multilayer system, it is very easy to fabricate, particularly in higher frequency regime where the complex 3D structures are relatively difficult to fabricate. As shown in Fig. 9a, the unit cell of the designed metamaterial contains two BC-SRR's, with one rotated by 90 degrees with respect to the other. To understand the resonance properties of the designed system, we employed FDTD simulations[84] to calculate the transmissions of EM plane waves with magnetic fields polarized along different directions and with different propagation directions[52]. The transmission spectra in different cases are compared in Fig. 9b. It is clearly shown that for **B** field along all three directions, a ***common*** resonance is excited at the frequency $\omega \sim 0.386\omega_u$, implying that the system exhibits strong responses to external magnetic fields along all three directions at this particular frequency.

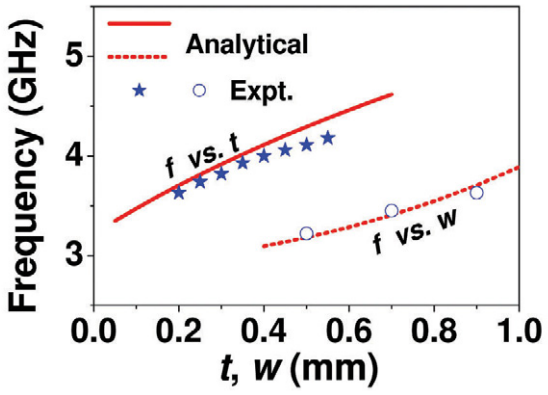

Fig. 8 SRR resonance frequency f (measured in GHz) as a function of t (setting $w = 0.9$ mm, solid line) and w (setting $t = 0.2$ mm, dotted line), calculated by our analytical formula. Symbols are experimental data taken from Figs. 7 and 8 of[36]. Reproduced from[51] with permission from the American Institute of Physics.

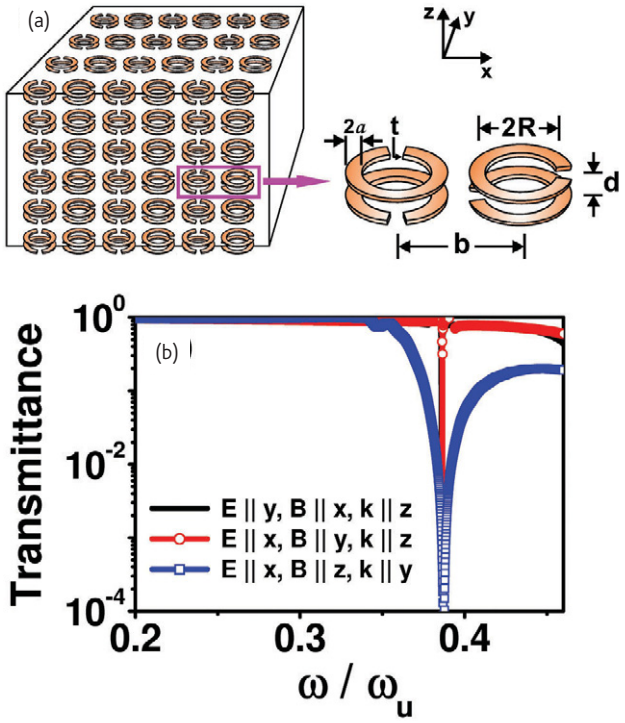

Fig. 9 (a) A schematic picture of the designed 3D magnetic material, with the inset showing the unit cell of structure. Here, $R = 4$ mm, $2a = 0.2$ mm, $t = 0.05$ mm, $d = 3$ mm, $b = 11$ mm and the gap width $\Delta = \pi/40$. (b) FDTD-calculated transmission spectra through the designed 3D magnetic material with different probing EM waves as specified in the figure. Reproduced from[52] with permission from the American Physical Society.

Conclusions

In this concise review, we have briefly summarized our recent efforts in establishing a rigorous mode-expansion theory and employing it to study the EM resonance properties of various SRR structures. The theory was established under the quasi-static limit and can be applied to study the resonance eigenmodes in *arbitrary* metallic ring systems, in which the inductive/capacitive effects were included completely and the relevant circuit parameters were calculated rigorously. The theory has been employed to study various SRR systems, including a single-ring SRR, a coplanar double-ring SRR and a broadside coupled SRR, and the obtained results are generally in good agreements with the FDTD simulations on realistic structures. We have also developed several analytical formulas, which agree well with FDTD and available experimental results, and might be useful for future metamaterial designs.

In a very recent work, Page *et al.*[89] established a theoretical approach which can also be applied to calculate all resonance frequencies of ring-like resonators. That approach can give additional physical insight into how geometry parameters affect the resonance frequencies by using the concepts of characteristic impedances and effective phase velocities[89]. However, that theory relies on finding a well-defined transmission-line description for

the structure and still needs some model parameters determined from other methods[89]. We believe that our theory and that one[89] are complementary in many aspects and are applicable to different situations.

While there have been lots of efforts to study the SRRs theoretically, we believe an analytical theory established on more rigorous grounds is still highly desirable, particularly since it can yield more physical insights and analytical formulas helpful for researchers working in this area. We look forward to more applications of our theory and extensions to other related problems. mt

Acknowledgements

This work was supported by the China-973 Program (2004CB719800), the NSFC (60725417, J0730310) and PCSIRT. STC is supported in part by the US DOE.

References

1. Veselago, V. G., *Sov. Phys. Usp.* (1968) **10**, 509.
2. Landau, L., and Lifschitz, E. M., Electrodynamics of Continuous Media, Elsevier, New York (1984).
3. Pendry, J. B., *et al., IEEE Trans. Microwave Theory Tech.* (1999) **47**, 2075.
4. Smith, D. R., *et al., Phys. Rev. Lett.* (2000) **84**, 4184.
5. Shelby, R. A., *et al., Science* (2001) **292**, 77.
6. Moser, H. O., *et al., Phys. Rev. Lett.* (2005) **94**, 063901.
7. Dolling, G., *et al., Opt. Lett.* (2007) **32**, 53.
8. Dolling, G., *et al., Opt. Lett.* (2006) **31**, 1800.
9. Zhang, S., *et al., Phys. Rev. Lett.* (2005) **95**, 137404.
10. Shalaev, V. M., *et al., Opt. Lett.* (2005) **30**, 3356.
11. Pendry, J. B., *Phys. Rev. Lett.* (2000) **85**, 3966.
12. Fang, N., *et al., Science* (2005) **308**, 534.
13. Ono, A., *et al., Phys. Rev. Lett.* (2005) **95**, 267407.
14. Belov, P. A., *et al., Phys. Rev. B* (2006) **73**, 033108.
15. Engheta, N., *IEEE Antennas Wireless Propag. Lett.* (2002) **1**, 10.
16. Zhou, L., *et al., Appl. Phys. Lett.* (2005) **86**, 101101.
17. Li, H., *et al., Appl. Phys. Lett.* (2006) **89**, 104101.
18. Li, J., *et al., Phys. Rev. Lett.* (2003) **90**, 083901.
19. Shadrivov, I. V., *et al., Phys. Rev. Lett.* (2005) **95**, 193903.
20. Sun, S., *et al., Phys. Rev. E* (2007) **75**, 066602.
21. Leonhardt, U., *Science* (2006) **312**, 1777.
22. Pendry, J. B., *et al., Science* (2006) **312**, 1780.
23. Schurig, D., *et al., Science* (2006) **314**, 977.
24. Klein, M. W., *et al., Science* (2006) **313**, 502.
25. Feth, N., *et al., Opt. Lett.* (2008) **33**, 1975.
26. Wang, B., *et al., Opt. Express* (2008) **16**, 16058.
27. O'Brien, S., *et al., Phys. Rev. B* (2004) **69**, 241101.
28. Zharov, A. A., *et al., Phys. Rev. Lett.* (2003) **91**, 037401.
29. Liu, Y., *et al., Phys. Rev. Lett.* (2007) **99**, 153901.
30. Dolling, G., *et al., Opt. Lett.* (2005) **30**, 3198.
31. Podolskiy, V. A., *et al., Opt. Express* (2003) **11**, 735.
32. Dolling, G., *et al., Science* (2006) **312**, 892.
33. Mary, A., *et al., Phys. Rev. Lett.* (2008) **101**, 103902.
34. Alù, A., and Engheta, N., *Phys. Rev. B* (2008) **78**, 085112.
35. Alù, A., *et al., Opt. Express* (2006) **14**, 1557.
36. Aydin, K., *et al., New J. Phys.* (2005) **7**, 168.
37. Radkovskaya, A., *et al., Microwave Opt. Technol. Lett.* (2005) **46**, 473.
38. Boulais, K. A., *et al., Appl. Phys. Lett.* (2008) **93**, 043518.
39. Aydina, K., and Ozbay, E., *J. Appl. Phys.* (2007) **101**, 024911.
40. Aydin, K., *et al., Opt. Express* (2004) **12**, 5896.
41. Sauviac, B., *et al., Electromagnetics* (2004) **24**, 317.
42. Shamonin, M., *et al., J. Appl. Phys.* (2004) **95**, 3778 .
43. Marqués, R., *et al., IEEE Trans. Antennas Propag.* (2003) **51**, 2572.
44. Aznar, F., *et al., Appl. Phys. Lett.* (2008) **92**, 043512.
45. Zhurbenko, V., *et al., Microwave Opt. Technol. Lett.* (2008) **50**, 511.
46. Shamonin, M., *et al., Microwave Opt. Technol. Lett.* (2005) **44**, 133.
47. García-García, J., *et al., J. Appl. Phys.* (2005) **98**, 033103.
48. Baena, J. D., *et al., Phys. Rev. B* (2004) **69**, 014402.
49. Marques, R., *et al., Phys. Rev. B* (2002) **65**, 144440.
50. Zhou, L., and Chui, S. T., *Phys. Rev. B* (2006) **74**, 035419.
51. Zhou, L., and Chui, S. T., *Appl. Phys. Lett.* (2007) **90**, 041903.
52. Huang, X. Q., *et al., Phys. Rev. B* (2008) **77**, 235105.
53. Chui, S. T., *et al., J. Appl. Phys.* (2008) **104**, 034305.
54. Katsarakis, N., *et al., Appl. Phys. Lett.* (2004) **84**, 2943.
55. Markos, P., and Soukoulis, C. M., *Phys. Rev. E* (2002) **65**, 036622.
56. Zhou, J., *et al., Phys. Rev. Lett.* (2005) **95**, 223902.
57. Yen, T. J., *et al., Science* (2004) **303**, 1494.
58. Linden, S., *et al., Science* (2004) **306**, 1351.
59. Zhou, J., *et al., Opt. Express* (2007) **15**, 17881.
60. Klein, M. W., *et al., Opt. Lett.* (2006) **31**, 1259.
61. Economou, E. N., *et al., Phys. Rev. B* (2008) **77**, 092401.
62. Zhao, Q., *et al., Appl. Phys. Lett.* (2007) **90**, 011112.
63. Enkrich, C., *et al., Phys. Rev. Lett.* (2005) **95**, 203901.
64. Bilotti, F., *et al., IEEE Trans. Antennas Propag.* (2007) **55**, 2258.
65. Azad, A. K., *et al., Appl. Phys. Lett.* (2008) **92**, 011119.
66. Smith, D. R., *et al., Appl. Phys. Lett.* (2000) **77**, 2246.
67. Smith, D. R., *et al., Phys. Rev. B* (2002) **65**, 195104.
68. Popa, B., and Cummer, S. A., *Phys. Rev. B* (2005) **72**, 165102.
69. Alicia, K. B., and Ozbay, E., *J. Appl. Phys.* (2007) **101**, 083104.
70. Little, B. E., *et al., J. Lightwave Technol.* (1997) **15**, 998.
71. Marques, R., *et al., Phys. Rev. Lett.* (2002) **89**,183901.
72. Xu, H., *et al., Appl. Phys. Lett.* (2008) **92**, 041122.
73. Wiltshire, M. C. K., *et al., Science* (2001) **291**, 849.
74. Wiltshire, M. C. K., *et al., Opt. Express* (2003) **11**,709.
75. Zhang, S., *et al., Phys. Rev. Lett.* (2005) **94**, 037402.
76. Verney, E., *et al., Phys. Lett. A* (2004) **331**, 244.
77. Baena, J. D., *et al., Appl. Phys. Lett.* (2006) **88**, 134108.
78. Baena, J. D., *et al., Appl. Phys. Lett.* (2007) **91**, 191105.
79. Baena, J. D., *et al., Phys. Rev. B* (2007) 76, 245115.
80. Gay-Balmaz, P., and Martin, O. J. F., *Appl. Phys. Lett.* (2002) **81**, 939.
81. Zhao, Q., *et al., Phys. Rev. Lett.* (2008) **101**, 027402.
82. Koschny, Th., *et al., Phys. Rev. B* (2005) **71**, 121103.
83. Jackson, J. D., *Classical Electromagnetic*, Wiley, New York (1999), 3rd edition.
84. CONCERTO 4.0, Vector Fields Limited, England, 2005.
85. Zedler, M., *et al., IEEE Trans. Micro. Theory Tech.* (2007) **55**, 2930.
86. Grbic, A., and Eleftheriades, G. V., *J. Appl. Phys.* (2005) **98**, 043106.
87. Alitalo, P., *et al., J. Appl. Phys.* (2006) **99**, 064912.
88. Vendik, I., *et al., Micro. Opt. Tech. Lett.* (2006) **48**, 2553.
89. Page, J. E., *et al., Int. J. Electron Commun. (AEU)* (2008), doi: 10.1016/j.aeue.2008.02.006